



Modeling of CO₂ transport and pressure buildup in reservoirs during CO₂ storage in saline aquifers: a case in Dongying Depression in China

Bo Liu^{1,2} · Jinpeng Xu¹ · Zhixiong Li^{3,4} · Reza Malekian⁵ · Zhimin Xu¹

Received: 5 September 2017 / Accepted: 29 January 2018 / Published online: 23 February 2018
© Springer-Verlag GmbH Germany, part of Springer Nature 2018

Abstract

Overuse of fossil fuels in industrial production and human life has increased greenhouse gas emissions. CO₂ geological storage in deep saline aquifer can effectively control the extensive emission of CO₂ and promote the smart cities performance of sustainability in economic, environmental, and social matters. The study area was set in the Dongying Depression, a structural unit of Bohai Bay. In this paper, four sets of reservoir and caprock layers suitable for CO₂ geological storage were selected for the analysis of the properties of saline aquifers and caprocks, from the Shahejie Formation layers, the Es₂, the upper and middle Es₃ layers at depths between 1464 and 3102 m. In order to assess the suitability and safety of CO₂ storage during and after the injection period in these four saline reservoirs, the simulation software TOUGHREACT was selected to simulate the CO₂ fluid migration process and pressure evolution in different conditions. The simulation results show that in the four reservoirs, the CO₂ plume migrated about 1000–1200 m, and the pressure increased in the whole reservoirs with the largest pressure increment of 0.552–1.749 MPa near the injection well during the CO₂ injection period; the CO₂ gradually dissolved in the reservoir water, and the pressure was quickly restored to the original pressure after the CO₂ injection period. The reservoir thickness, the porosity, and the permeability have an effect on the CO₂ migration movement, and the pressure evolution in the reservoir, the shallower, and thicker reservoir is comparatively more suitable for CO₂ geological storage. The sensitivity analysis proved the significant effect of the porosity and permeability on the CO₂ transport and reservoir pressure. The results will be helpful to guide the development of CO₂ geological storage projects and provide the theoretical basis for CO₂ storage risk monitoring.

Keywords Modeling · CO₂ transportation · Pressure buildup · CO₂ storage · Saline aquifers

Introduction

The concept of Smart Cities has become an increasingly common trend in technology-based projects (De Paz et al. 2016). Balancing the environment and natural resources is a practical and responsible way to ensure that the environment and resources on the planet are conserved appropriately for the next generation. Geological sequestration is a good means of reducing anthropogenic atmospheric emissions of CO₂ that is immediately available and technologically feasible. Three kinds of geological settings have been recognized as major potential CO₂ sinks: deep saline-filled sedimentary formations, depleted oil and natural gas reservoirs, and un-mineable coal seams (Bradshaw et al. 2007; Brown et al. 2014; Gislason and Oelkers 2014; Abidoye et al. 2015; Du et al. 2016). However, the geological sequestration in saline aquifers is considered a most viable option as it seems

✉ Bo Liu
boliu@cumt.edu.cn

¹ School of Resources and Geosciences, China University of Mining and Technology, Xuzhou 221116, China

² Scientific Research Foundation of Key Laboratory of Coal-Based CO₂ Capture and Geological Storage, Jiangsu Province, China University of Mining and Technology, Xuzhou 221008, China

³ School of Mechatronics Engineering, China University of Mining and Technology, Xuzhou 221116, China

⁴ School of Manufacturing and Mechanical Engineering, UNSW, Sydney 2200, Australia

⁵ Department of Electrical, Electronic and Computer Engineering, University of Pretoria, Pretoria 0002, South Africa

to have very large carbon storage potential (Bachu 2008; Zahid et al. 2011; Zheng et al. 2013). Parts of the reasons for this include the stability, capacity, and ubiquity of these aquifers (Bachu 2015). Stable sedimentary basins are necessary for dependable sequestration, and such basins are found in most continents with estimated capacities of around 1000–100,000 gigatonnes of CO₂ (Zahid et al. 2011).

One of the primary concerns in CO₂ sequestration is the safety and long term of CO₂ immobilization. There are mainly four storage mechanisms for immobilizing CO₂ in a porous medium: structural trapping, residual trapping, dissolution trapping, and mineral trapping (Xu et al. 2005; Bachu 2008; Zhang et al. 2009; Hidalgo et al. 2013; Martinez-Landa et al. 2013). When CO₂ is injected into the subsurface, it is first trapped by the first two storage mechanisms (Bachu 2008). During this period, the CO₂ existing as a free phase in the reservoir pore space would not dissolve quickly in groundwater, which would cause CO₂ transportation and pressure buildup in the reservoir and increase the risk of CO₂ leakage (Yang et al. 2014, 2015; Meng et al. 2015).

Studying and modeling CO₂ sequestration in geological formations need a clear understanding of multiphase flow characteristics and its behavior in porous media. Briefly, CO₂ was injected into a formation at high flow rate through an injection well. The supercritical CO₂ fluid flowed into the relatively more permeable regions surrounding the well and displaced native formation water under strong pressure gradients (e.g., brine) (Birkholzer et al. 2015). The CO₂ injected at the bottom of the storage formation migrates upward rapidly by buoyancy forces because the density of the supercritical CO₂ phase is lower than that of the aqueous phase. A small fraction of CO₂ gas is trapped in the porous rock as a residual gas after injection, and most of the free CO₂ gas accumulates below the caprock, forms a CO₂ plume, and is transported far away (Zhang et al. 2009). The spreading and migration of mobile CO₂ could increase the risk of CO₂ leakage into shallower formations through fractures, outcrops, or abandoned wells (Lewicki et al. 2007; Lu et al. 2010). Moreover, the increased pressures caused by CO₂ injection in the storage formations could induce geomechanical alteration of the reservoirs and their surroundings, for example, creating new fractures or reactivating larger faults (Rutqvist 2012). These changes taking place in the caprock or overburden could result in new leakage pathways for brine and/or CO₂. If such leakage cannot be properly assessed, geological sequestration of CO₂ might lead to undesirable environmental and safety consequences that may ultimately prevent future deployment of geological sequestration of CO₂ (Jung et al. 2015). Therefore, flow barriers, such as faults, increase induced pressure considerably; for reservoirs with such features, careful site characterization and operational planning will be required for large storage projects (Chadwick et al. 2009).

Many researchers have significantly improved the knowledge base and addressed many of the technical gaps in CO₂ storage. A large body of research has been devoted to identify and verify the main processes that control CO₂ migration, trapping, and containment in deep saline aquifers. However, less attention has been paid to the effects of pressure buildup associated with CO₂ injection (Birkholzer et al. 2015).

In this study, four sets of reservoirs suitable for CO₂ storage in deep saline aquifers in Dongying Sag with different conditions were selected and analyzed. CO₂ plume behavior and pressure buildup in different reservoirs, which are extremely important to CO₂ storage safely, were analyzed using numerical simulation by TOUGHREACT. In this study, an attempt is made to provide an important basis for carrying out the actual CO₂ injection project in the future.

Geological and hydrogeological setting

Geological background

The Dongying Sag is a sub-tectonic unit lying in the southeastern part of the Jiyang Depression of the Bohai Bay Basin (Cao et al. 2014). It is a Mesozoic–Cenozoic half graben-like basin that is bounded to the east by the Qingtuozui Bulge, to the south by the Luxi Uplift and Guangrao Bulge, to the west by the Gaoqing Fault, and to the north by the Chenji-zhuang–Binxian Bulge (Fig. 1). The Dongying Sag covers an area of 5700–5850 km² with an east–west axis of 90 km and a north–south axis of 65 km (Cao et al. 2014; Wang et al. 2016). The tectonic evolution of the Dongying Sag can be subdivided into three stages: the rifting, faulting, and depression stages. During the rifting period, the Dongying Sag was affected by intensive structural uplift with soils developed, mainly in alluvial fans and deltas. In the faulting stage, sediment deposition was effected by tectonic activity, paleoclimatic changes, and sediment supply. With declining tectonic activity, lakes shrank gradually, forming monospecific facies dominated by fluvial facies in the depression stage (Li and Li 2016). The sag is filled with Cenozoic sediments, which are formations from the Paleogene, Neogene, and Quaternary periods. The formations from the Paleogene period are the Kongdian (Ek), Shahejie (Es), and Dongying (Ed); the formations from the Neogene period are the Guantao (Ng) and Minghuazhen (Nm); and the formation from the Quaternary period is the Pingyuan (Qp) (Guo et al. 2012; Zhang et al. 2004, 2010).

Hydrogeological background

Palaeohydrogeology and hydrogeochemistry of water-bearing rock series in Dongying Sag are divided into different periods

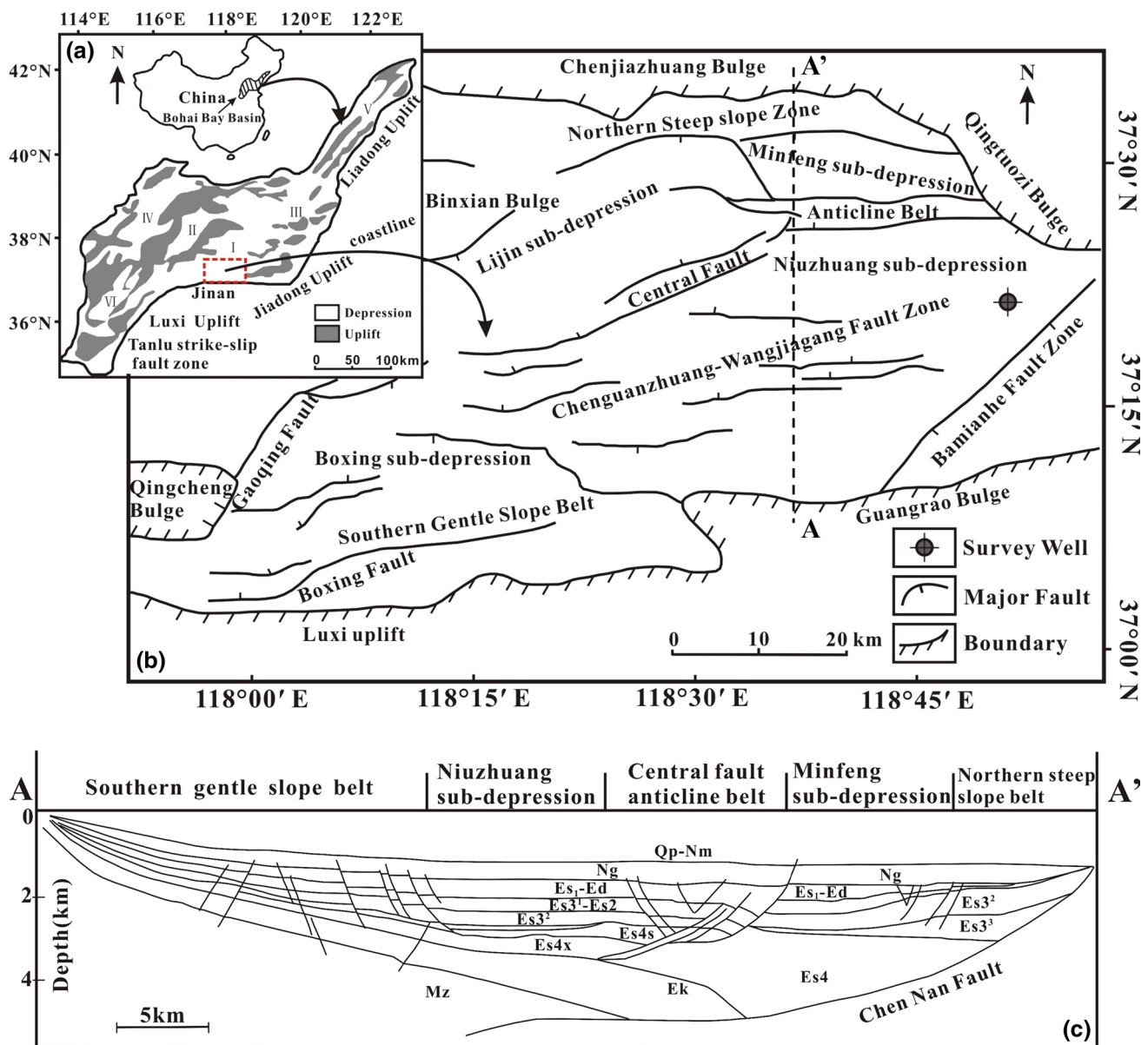


Fig. 1 Location of the Dongying Depression (**a** Position and structure of Bohai Bay Basin, (I) Jiyang subbasin, (II) Huanghua subbasin, (III) Bozhong subbasin, (IV) Zhezong subbasin, (V) Liaohu subbasin, (VI) Dongpu subbasin; **b** Structural units of Dongying Depres-

sion; **c** Cross section (A–A') showing the various tectono-structural zones and key stratigraphic intervals within the Dongying Depression) (Modified from Guo et al. 2012)

through the combination of hydrogeological cycle with hydrogeological period. Atmospheric water infiltrates from the edge of the depression to the center forming a centripetal flow. The mudstone-compacted water migrates from the center of the depression to the surrounding forming a centrifugal flow. The groundwater drains to southern slope, northern fault zone, and the central fault zone (Yang 1985). Mudstone-compacted water is an important source of sedimentary groundwater and controls the hydrodynamic field formation and evolution of the Dongying Sag (Xie and Wang 1998). Lateral movement of the compacted water in the Tertiary Shahejie Formations

is extremely slow, and such a low flow rate is essentially close to still water. The formation water salinity is generally 15,700–26,817 mg/L, and the hydrochemical types of groundwater in Shahejie Formations are mainly CaCl₂ type, and secondly NaHCO₃ type.

Numerical approaches

Numerical tool

Following Xu et al. (2006, 2011), we conducted the numerical simulations by TOUGHREACT, a program being applied to the study of non-isothermal multiphase reactive geochemical transport. TOUGHREACT was produced on the base of TOUGH2 V2—the multiphase fluid and heat flow code developed by Pruess et al. (1999, 2004), with the introduction of reactive geochemistry (Zhang et al. 2009; Xu et al. 2010). Please see *TOUGHREACT User’s Guide* for the specific information (Xu et al. 2012).

Model setup

Hydrogeological conceptual model

The test results of 154 core and water samples from an exploration well in the study area showed the Shahejie Formation consists of interbedded layers of sand rocks and mudstones, with a suitable thickness and good stability of each layer. Among the Shahejie Formation layers, Es2, the upper and middle Es3 layers with a burial depth of 1464–3102 m, there are four sets of reservoirs suitable for CO₂ storage, shown in Fig. 2. The reservoirs are sand rocks, with appropriate depth, thickness, porosity and permeability. The groundwater in these aquifers is saline water, with a salinity of 15,700–26,817 mg/L. The specific parameters for the four reservoirs are summarized in Table 1. Above each reservoir, there is a layer of comparatively impermeable mudstone as caprock to

Fig. 2 Stratigraphic column of the site for CO₂ storage

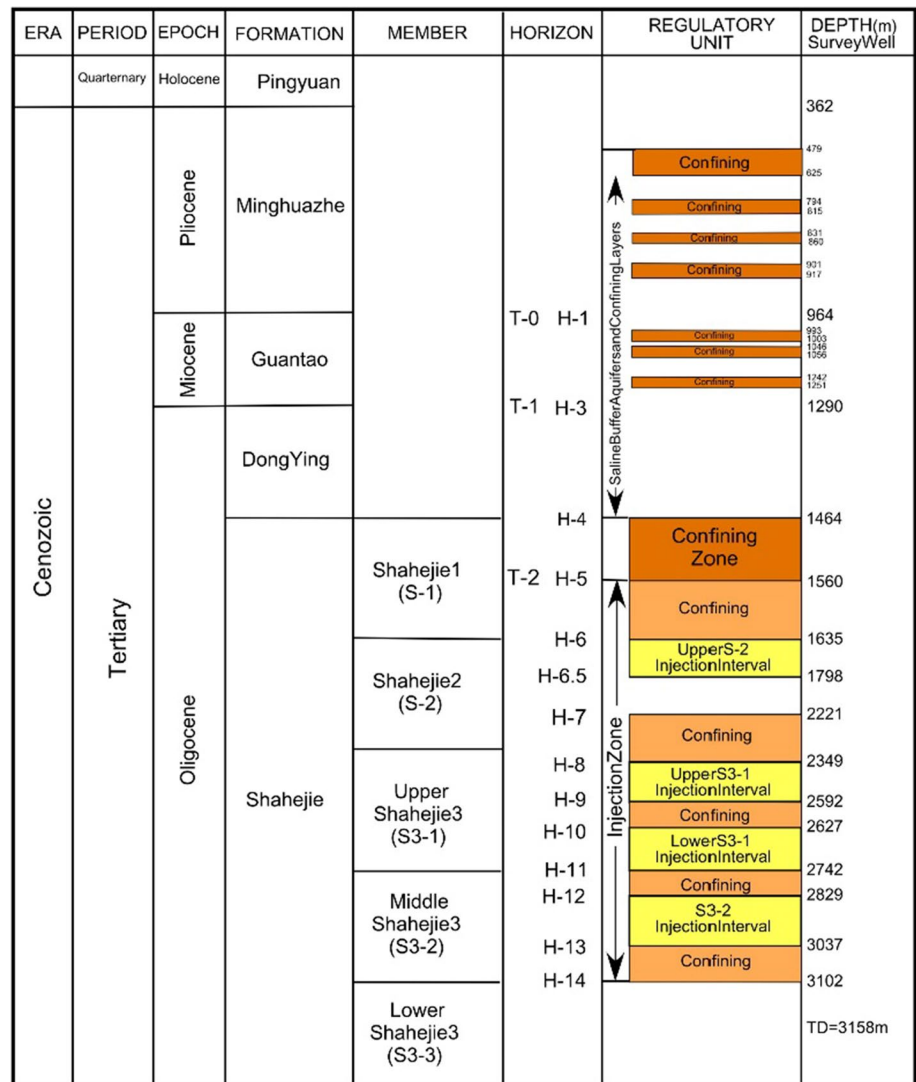


Table 1 Properties of the four reservoirs for CO₂ geological storage

No.	Lithology	Roof depth (m)	Cumulative thickness (m)	Effective thickness (m)	Porosity (%)	Permeability (mD)	Salinity (mg/L)
1	Sand	1637.4	198	110.1	26.4	517.9	24,075
2	Sand	2351.5	243.2	202.4	24.0	410.0	15,700
3	Sand	2628.2	80	77.3	21.5	266	21,900
4	Sand	2831.1	208.2	148.4	16.7	115.9	26,817

Table 2 Properties of the four caprocks for CO₂ geological storage

No.	Lithology	Roof depth (m)	Cumulative thickness (m)	Effective thickness (m)	Continuous thickness (m)
1	Mud	1465.4	147.8	71	16
2	Mud	2160	189	180	100
3	Mud	2592	35	35	35
4	Mud	2742	87	70	38

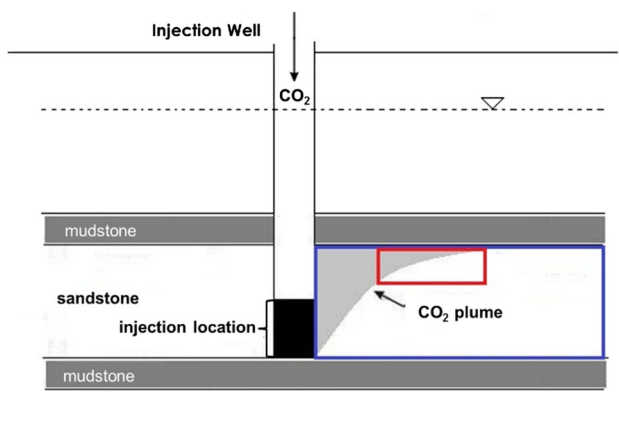


Fig. 3 Schematic diagram for CO₂ storage in deep saline aquifer

prevent CO₂ from leaking out of the reservoirs. The specific parameters for the four caprocks are summarized in Table 2. Besides, above the Shahejie Formation, there are some thin mudstones as buffer layers in the Minghuazhen and Guantao Formations to ensure CO₂ storage in deep saline aquifers.

Because of the pure lithology and stable deposition of the study area, the reservoirs were assumed to be horizontal homogeneous sandstone aquifers, the thicknesses of which were stable. Considering the vertical pressure during the development of strata, the reservoirs were assumed to be anisotropic, and the ratio of vertical to horizontal permeability is 0.1. Two layers of mudstones, respectively, overlie and underlie the sandstone reservoir. CO₂ is injected into the reservoir from a well, and the CO₂ outlet is located in the half bottom portion of the well. Therefore, a generalized

hydrogeological conceptual model of taking these features into account is of the form shown in Fig. 3.

Boundary and meshing

Based on the above-mentioned hydrogeological conceptual model, a simple two-dimensional (R–Z, 2D) radial model was used to simulate the CO₂ plume migration and pressure buildup during and after injecting CO₂ into the reservoirs. According to the area and the shape of Dongying Depression, the simulated range is generalized to a circle with a radius of 77,500 m. For each reservoir, 101 radial grid elements with spacing increasing gradually away from the injection well were used in the horizontal direction. Different numbers of vertical grid elements but with a constant spacing of 10 m were used in the vertical direction with reference to the specific thickness of the four reservoirs. The injection well is a flow boundary with a constant CO₂ injection rate of 5 kg/s 10 m at half of the well, which is located on the Z-axis. Upper and lower mudstone layers are impermeable boundaries. Lateral is an infinite boundary, which was reflected in the model by giving the outer grid element a large volume of 10³⁰ m³.

Simulation parameters

In the model, three types of parameters were input, including hydrogeological conditions, initial minerals, and water chemical composition of the reservoirs. Hydrogeological conditions of the four reservoirs were different due to their different depths, shown in Table 3. The values of thicknesses, porosity, and permeability are assigned with reference to the core test data. The values of temperature are assigned according to the average depth for the specific

Table 3 Hydrogeological parameters used in the simulations

Parameters	Reservoir 1	Reservoir 2	Reservoir 3	Reservoir 4
Thickness (m)	110	200	80	150
Porosity	0.264	0.240	0.215	0.167
Permeability, k_v/k_h (m^2)	51.79/517.90	40.00/400.00	22.60/226.00	11.59/115.90
Temperature ($^{\circ}C$)	75	102	110	142
Pressure ($\times 10^7 Pa$)	1.64	2.35	2.63	2.83
Compressibility (Pa^{-1})	4.5×10^{-10}	4.5×10^{-10}	4.5×10^{-10}	4.5×10^{-10}
Residual water saturation	0.30	0.30	0.30	0.30
Residual gas saturation	0.05	0.05	0.05	0.05

reservoir with a geothermal gradient of $3.6^{\circ}C/100$ m and the average annual surface temperature of $14^{\circ}C$ (Yang 1984). The values of pressure are assigned according to the average depth for the specific reservoir with a usual pressure gradient of 1 MPa/100 m. Values of compressibility, residual water saturation, and residual gas saturation are assigned according to the properties of sandstone (Zhou et al. 2008; Birkholzer et al. 2009; Zhang et al. 2009; Shevalier et al. 2011; Xu et al. 2011; Beni et al. 2012). The initial mineral composition and water chemical composition of the four reservoirs were the same, because they were all sandstone reservoirs of the Shahejie Formation (As we do not discuss chemical reactions in this paper, the specific data are not shown here).

Results and discussion

Though the hydrogeochemical reaction among CO_2 , rock, and brine was considered in the simulations, we discuss here mainly the CO_2 plume migration and the pressure buildup by CO_2 injection, which are vitally important to safe CO_2 storage in deep saline reservoirs. And these two processes are mainly controlled by the physical properties of reservoirs including depth (which determines the reservoir temperature and pressure), thickness, porosity, and permeability. The simulation period up to 1000 years includes an injection period of 10 years and an after injection period of 990 years.

CO_2 migration in different reservoirs

During the CO_2 injection period, CO_2 displaces the formation water in the pore volumes, and the displaced water flows into the surroundings. The injected CO_2 moves upward by buoyancy and simultaneously moves laterally by injection pressure. Thus, a drainage zone was formed and spread out in the shape of a CO_2 plume in the four reservoirs (Fig. 4). Especially, in the vicinity of the injection well, the saturation of the formation water was zero. A larger drainage zone of less porosity and permeability was formed in the reservoir; for example, after injecting CO_2 for 10 years, the

range of the dry out zone in the fourth reservoir was the largest (Fig. 4p). This is mainly because the rock pore volume of a reservoir with smaller permeability and porosity can be quickly filled with CO_2 . In other words, injecting the same volume of CO_2 , the distribution of the CO_2 plume in a smaller porosity reservoir was wider.

The radial distance of CO_2 migration at the bottom of the fourth reservoir (Fig. 4d, h, l, p) was obviously farther than that in the other three reservoirs. This is because CO_2 injection can cause a rock pore pressure increase, the rock pore pressure increased more in reservoirs with a smaller porosity. Moreover, as the ratio of vertical permeability to horizontal permeability was set to 0.1, CO_2 was easier to move in the horizontal direction in the reservoirs with a small porosity. Thus, when the reservoir pore pressure increases, radial distance of CO_2 migration at the bottom in a reservoir with a smaller permeability was larger than that in a reservoir with a greater permeability.

In the early period of CO_2 injection, in the reservoirs with similar porosities and permeabilities, the radial distance of CO_2 migration in the upper part of a thin reservoir was greater than that in the upper part of a thick reservoir. In Fig. 4, it is seen that after injecting CO_2 for 1 year, the radial distance of CO_2 migration was about 200 m in the upper part of the first reservoir (Fig. 4a), while CO_2 just migrated up to the top of the second reservoir (Fig. 4b). This is mainly because in the thin reservoir, CO_2 was first vertically transported to the top of the reservoir and then horizontally migrated in the radial direction; however, in the thick reservoir, CO_2 should migrate upward over a long distance and take more time to reach the top of reservoir.

In the CO_2 injection period of 10 years, the CO_2 plume front migrated approximately 1200, 1200, 1000, and 1000 m downward in the four reservoirs.

After injection, the buoyant CO_2 will further spread upward and migrate laterally. As no new CO_2 is injected into the reservoirs, the early injected CO_2 gradually began to dissolve in the formation water (Fig. 5). In the first and second reservoirs, most of the injected CO_2 dissolved after the CO_2 injection period of 20 years (Fig. 5a, b). However, a fair portion of the CO_2 still existed as a gas phase in the third

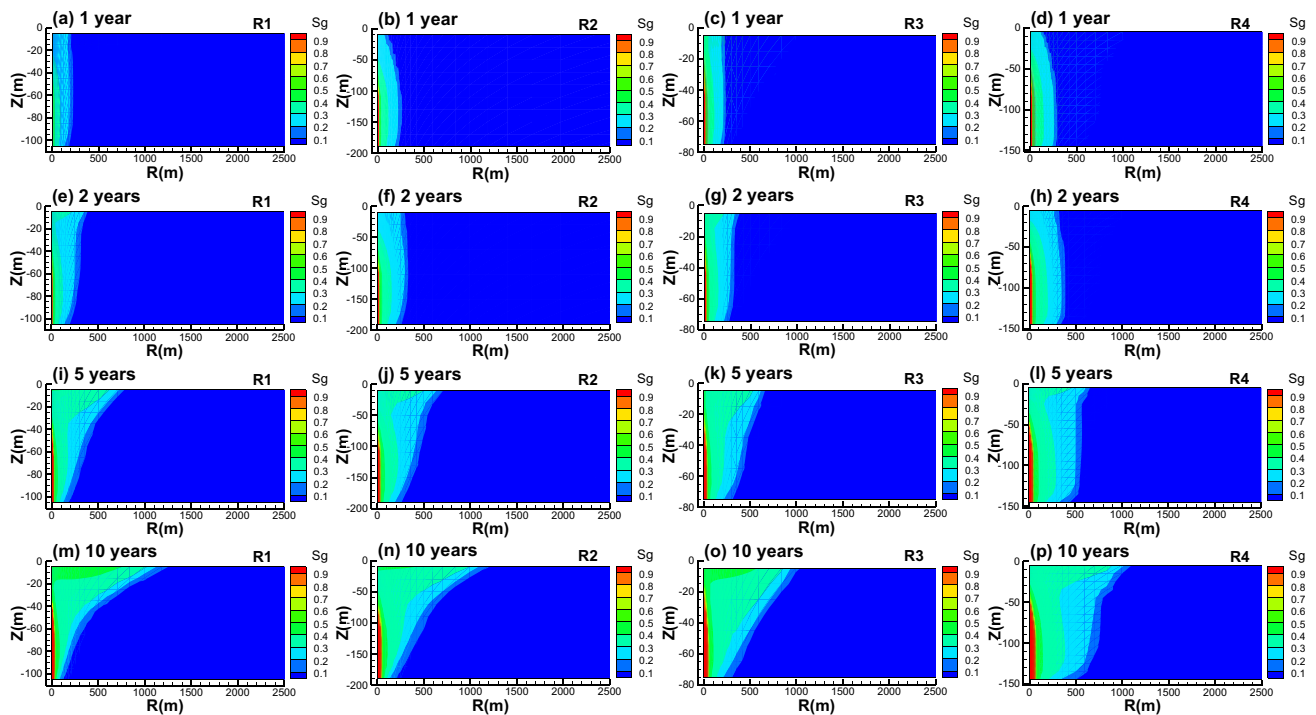


Fig. 4 Spatial distribution of CO₂ gas saturation during the CO₂ injection period for the four reservoirs

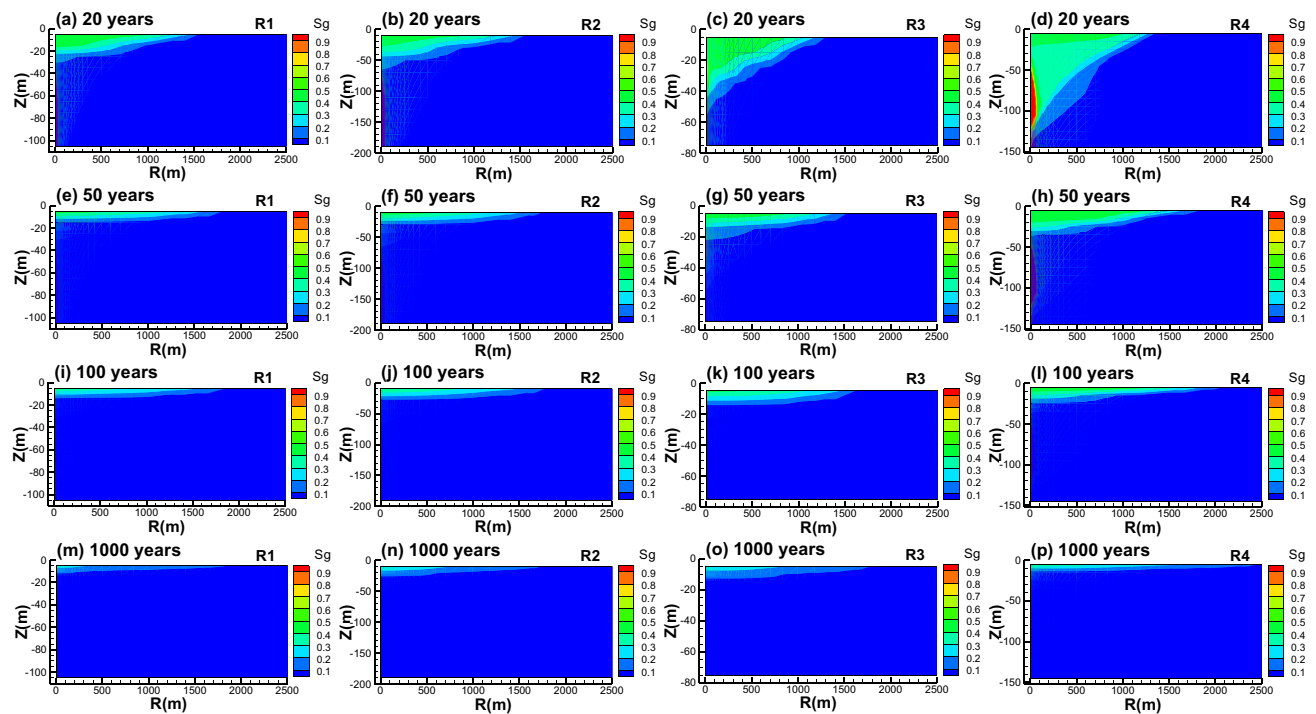


Fig. 5 Spatial distribution of CO₂ gas saturation after the CO₂ injection period for the four reservoirs

and fourth reservoirs (Fig. 5c, d), especially in the fourth reservoir. This is because CO₂ could migrate easily and have a large contact area with brine in reservoirs with a great

porosity and permeability, which promoted the dissolution of CO₂ in saline water, and CO₂ could not dissolve quickly in the reservoirs with a small porosity and permeability. After

a CO₂ injection period of 1000 years, almost all the CO₂ dissolved in the four reservoirs (Fig. 5m–p).

Pressure buildup in different reservoirs

Before CO₂ injection, the pressure at the same depth is the same for each reservoir (Fig. 6a–d). Because of different depths and thicknesses of the four reservoirs, the pressure ranges and the contour legend levels in the figures are also different for the four reservoirs simulated.

When injecting CO₂ into saline aquifers, the pressure fields for the four reservoirs changed. At the beginning, the pressure near the injection well increased immediately. With increased injection time, the pressure buildup zone was extended. Since the original reservoir is completely filled with groundwater, CO₂ injection resulted in an instantaneous pressure increase near the injection well, and the influence zone spread far away from the location of the well. The pressure increased in magnitude close to injection well was greater than away from it (shown in Fig. 6e–t).

In the reservoirs with similar porosities and permeabilities, the radial range of pressure buildup in a thick reservoir

was smaller than that in a thin reservoir. As shown in Fig. 6e, f, the thickness of the first reservoir is only half that of the second reservoir, and the zone of pressure buildup in the first reservoir was larger than that in the second reservoir. This is mainly because the CO₂ injected into reservoir first moves upward by buoyancy. A thick reservoir has a high capacity to relieve the increased pressure in a vertical direction. A thin reservoir was limited by thickness, and CO₂ should move more in a radial direction to relieve the increased pressure.

The pressure buildup by injecting CO₂ was mostly affected by reservoir porosity and permeability. The pressure increased in magnitude, and the spread range was larger in a reservoir with small porosity and permeability than that in a reservoir with large porosity and permeability. As shown in Fig. 6h, l, p, t, the pressure increased in magnitude and the distribution range was larger in the fourth reservoir than the other three reservoirs. This is because groundwater flows slowly in a reservoir with a small porosity and permeability, and during CO₂ injection, the pore pressure increased drastically and formed a large pressure gradient.

The distance of pressure propagation was nearly up to the boundary after a CO₂ injection of 10 years in the four

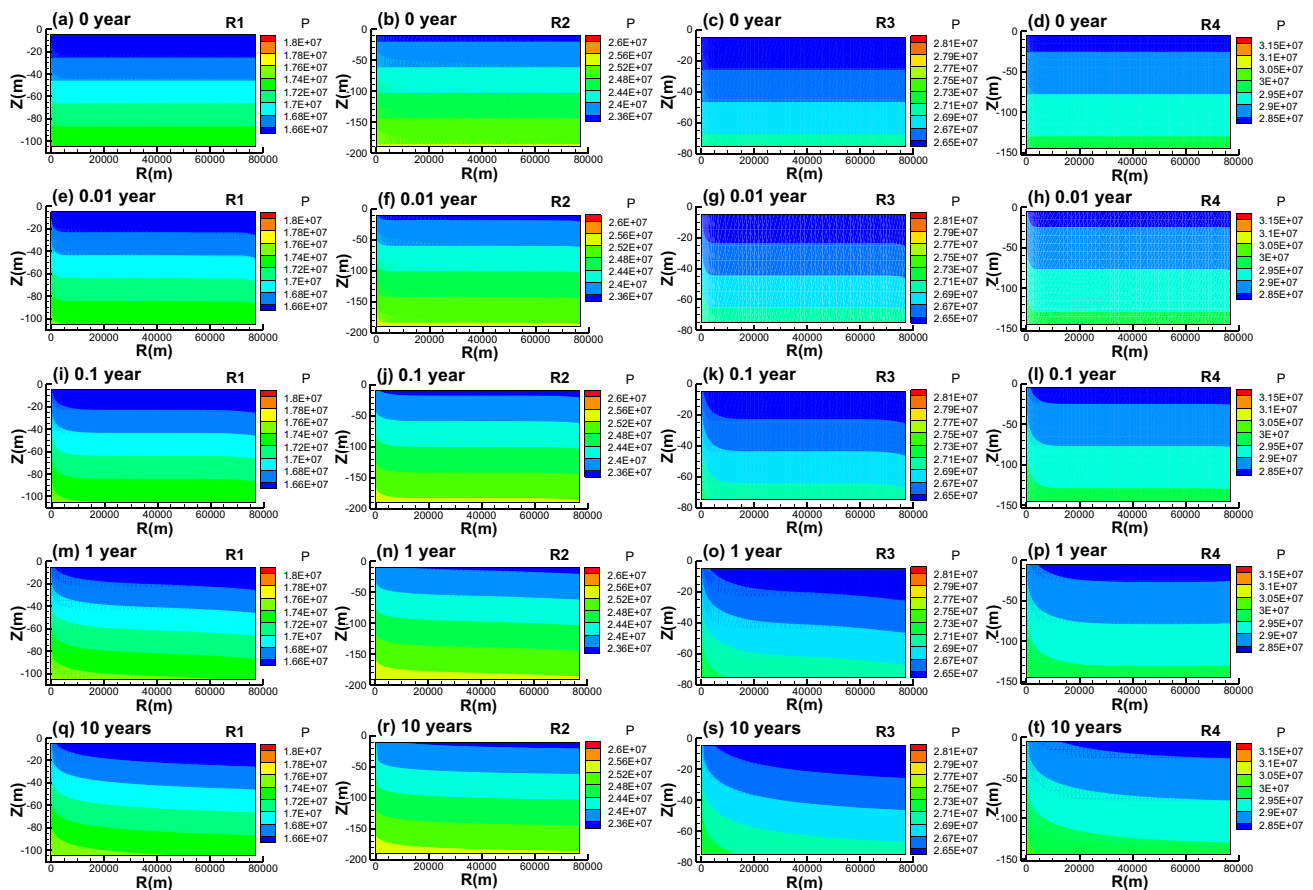


Fig. 6 Spatial distribution of the pressure buildup during the CO₂ injection period

reservoirs (Fig. 6q–t), especially in the third and fourth reservoirs, greater than the distance of CO₂ plume migration, which indicated that the range of pressure increase caused by CO₂ injection was far away from the injection well and much wider than the range of CO₂ storage location in the reservoir.

After CO₂ injection, the pressure in the four reservoirs began to recover (Fig. 7). Pressure recovery can be explained in two ways: On the one hand, the increased pressure transferred far away (lateral was defined as an infinite boundary in the model) and on the other hand, a large amount of CO₂ dissolved in the reservoir water. After a CO₂ injection period of 1000 years, the pressures in the four reservoirs recovered to each one’s original levels.

In order to further evaluate the safety of storage CO₂ in the four reservoirs, the pressure changes in different locations in each reservoir and at different times during the CO₂ injection period were analyzed. As shown in Fig. 8 and Table 4, pressure changes in different locations of the four reservoirs reflected the same pattern with injection time.

For the four reservoirs, the pressure increment tends to decrease away from the injection well in a radial direction. This is because the thickness of the CO₂ plume gradually

decreases from the injection well to a location far away from the well. And the undissolved CO₂ in the reservoir can greatly increase the pore pressure.

Close to the injection well, the pressure increment in the upper layer was smaller than that in the lower layer. At the location about 200 m away from the injection well, the pressure increment in the upper layer was greater than that in the lower layer. And at the location about 2000 m away from the injection well, the pressure increment in the upper layer was as large as that in the lower layer. This phenomenon can be explained by assuming that near to injection well the CO₂ was continuously injected into the lower half of the well, and the CO₂ cannot dissolve or move upward quickly, and this causes the pressure increment in lower layer to be greater than that in the upper layer; at the location not far away from the injection well, the CO₂ gradually dissolved or moved upward, which leads to the pressure increment in upper layer being greater than that in the lower layer at the location about 200 m away from the injection well; and at the location far away from the injection well, there was no undissolved CO₂ and the pressure increment was mainly caused by a lateral pressure transmission, therefore, the

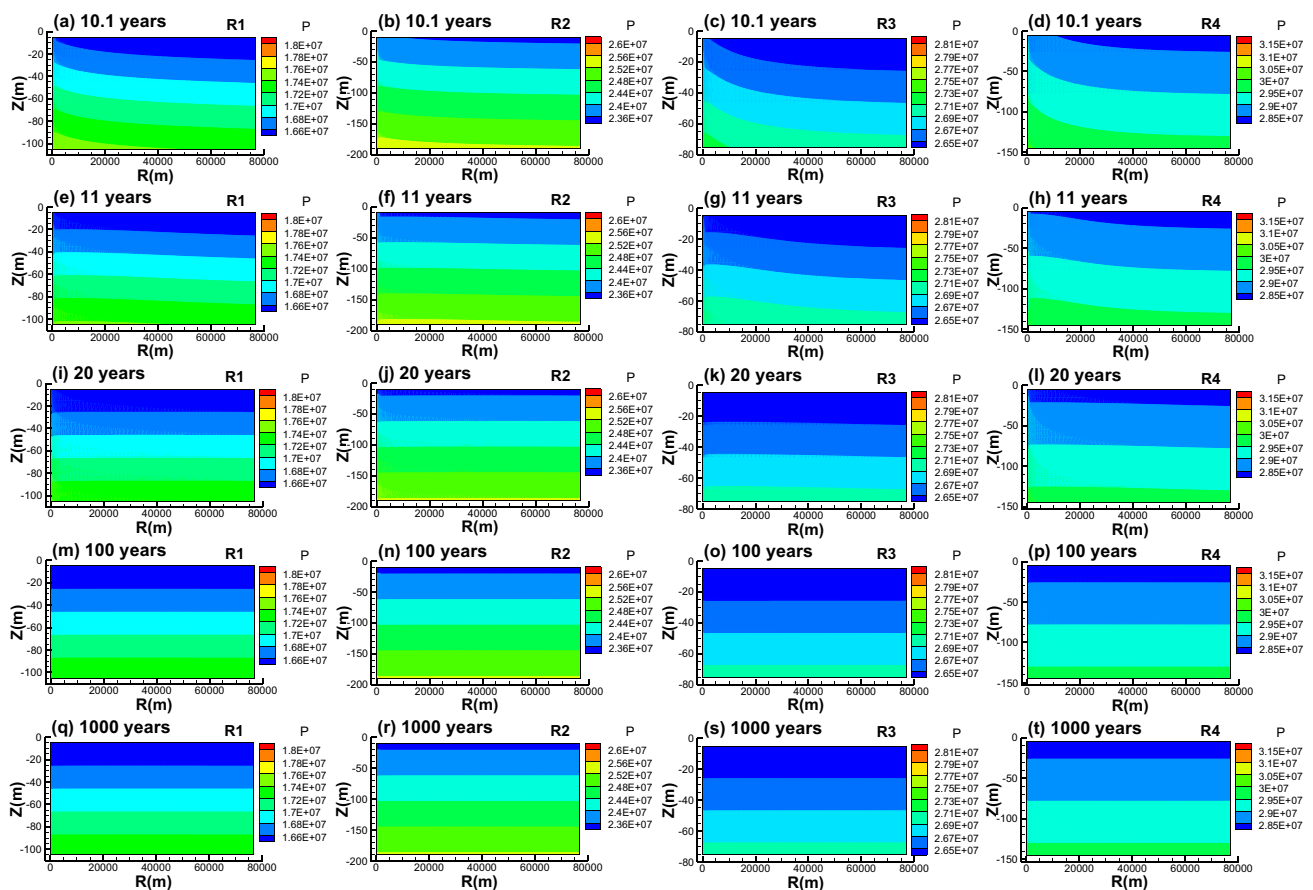


Fig. 7 Spatial distribution of the pressure dissipation after the CO₂ injection period

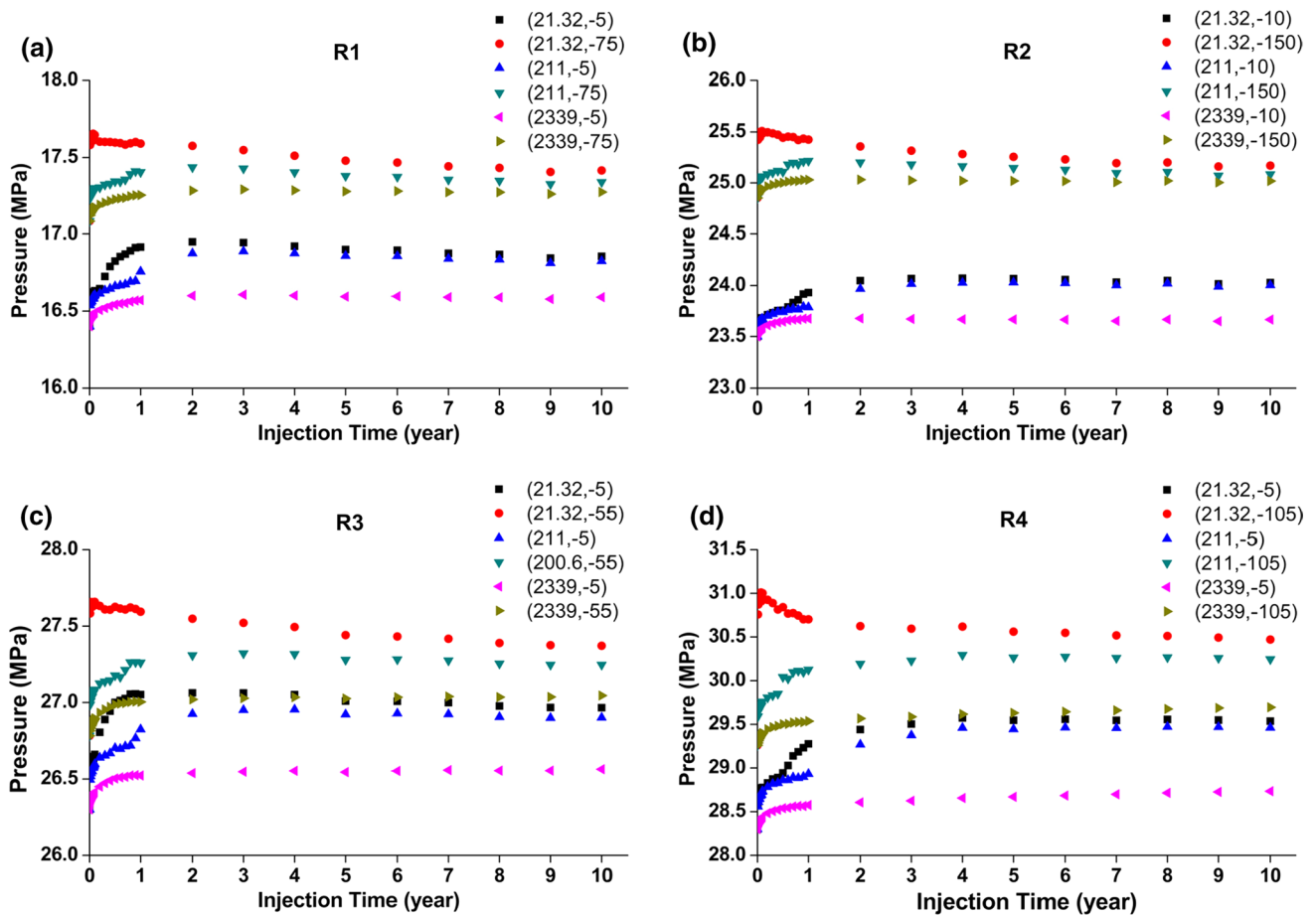


Fig. 8 Changes in the pressure in different locations of the four reservoirs with injection time [where (21.32, - 5) represents the location 21.32 m away from injection well, and 5 m below the top of the reservoir, and so forth for others]

pressure increment in the upper layer was as great as that in the lower layer.

For the same location in different reservoirs, the pressure increment in the lower reservoir was larger than that in the upper reservoir. This is because the porosity and permeability of the lower reservoir were smaller than those of the upper reservoir. As the amount of CO_2 injected into the unit thickness reservoir was equal, the CO_2 injected into the lower reservoir with a smaller porosity and permeability could increase the pore pressure greatly.

Sensitivity analysis

In order to analyze the numerical model sensitivity to the parameters of reservoir porosity, permeability, and thickness, based on the parameters of the first reservoir, we, respectively, changed the value of porosity to 0.167, the value of permeability to 115.9 mD, and the value of reservoir thickness to 200 m.

The effect of different parameter values on the CO_2 transport is represented in Fig. 9. Porosity and permeability

have a significant impact on the CO_2 migration. Compared with the CO_2 plume distribution of original first reservoir (Fig. 9a, e, i, m), the CO_2 moves farther in the upper reservoir when the value of porosity is reduced (Fig. 9b, f, j, n), and the CO_2 moves farther in the lower reservoir when the value of permeability is reduced (Fig. 9c, g, k, o). The thickness of reservoir has little effect on the CO_2 plume distribution (Fig. 9d, h, l, p).

The effect of different parameter values on the reservoir pressure transport is represented in Fig. 10. Permeability has a great influence on reservoir pressure. Compared with the pressure of original first reservoir (Fig. 10a, e, i, m), the pressure increased much when the value of permeability is reduced (Fig. 10c, g, k, o). The porosity and the thickness of reservoir affect the reservoir pressure little (Fig. 9b, f, j, n, d, h, l, p).

Limitation discussion

The geological model was simplified to a circle in the plane according to the area and the shape of Dongying Depression,

Table 4 Pressure changes in different position in the four reservoirs

Reservoir	Location	Near to injection well			In the middle of the layer			Far away from injection well			
		Initial pressure (MPa)	Maximum pressure (MPa)	Corresponding time (year)	Pressure increment (MPa)	Maximum pressure (MPa)	Corresponding time (year)	Pressure increment (MPa)	Maximum pressure (MPa)	Corresponding time (year)	Pressure increment (MPa)
R1	Upper	16.400	16.952	2	0.552	16.891	3	0.491	16.607	3	0.207
	Lower	17.084	17.655	0.07	0.571	17.436	2	0.352	17.291	3	0.207
R2	Upper	23.500	24.071	4	0.571	24.031	5	0.531	23.678	2	0.178
	Lower	24.854	25.508	0.09	0.654	25.217	1	0.363	25.032	2	0.178
R3	Upper	26.300	27.063	2	0.763	26.954	4	0.654	26.557	7	0.257
	Lower	26.782	27.658	0.1	0.876	27.321	3	0.539	27.039	7	0.257
R4	Upper	28.300	29.573	4	1.273	29.472	8	1.172	28.734	10	0.434
	Lower	29.260	31.009	0.07	1.749	30.294	4	1.034	29.695	10	0.435

and the outer boundary of the model was given at the edge of Dongying Depression. It did not consider the influence of faults, since there was not enough information to confirm the location and conductivities of the faults. And this study mainly focuses on the effect of reservoir porosity, permeability, and thickness on the CO₂ migration and reservoir pressure buildup.

Currently, operational data are not available to fully calibrate the numerical model though laboratory experiment. But the numerical software used in this study has been widely recognized in CO₂ geological storage (Xu and Pruess 2001). We will compare the numerical model results to some basic analytical solutions or real field data to further prove that the simulation results are reasonable in the future research.

Conclusions

In the study area of Dongying Sag, there are four sets of reservoirs suitable for CO₂ storage. The reservoirs are all made of sandrock, but at different depth, thickness, porosity, and permeability. During the CO₂ injection period, a drainage zone was formed and spread out in the shape of a CO₂ plume in the four reservoirs. The migration of CO₂ plumes was mainly controlled by the porosity and permeability of the reservoirs. For the same injection time and an equal amount of CO₂ injection per unit thickness, the radial distance of CO₂ migration at the bottom of a reservoir of smaller porosity and permeability was wider than that in a reservoir of greater porosity and permeability. In the early period of CO₂ injection, the radial distance of CO₂ migration in the upper part of a thin reservoir was greater than that in the upper part of a thick reservoir. In the late period of CO₂ injection, the radial distance of CO₂ migration in the upper part of a thick reservoir was larger than that in the upper part of a thin reservoir. After CO₂ injection period, CO₂ gradually moves upward and is transported laterally along the upper parts of the reservoirs, and almost all the CO₂ is dissolved in the reservoir water after 1000 years.

Injecting CO₂ into saline aquifers caused an increase in the reservoir pressure. The pressure buildup by CO₂ injection was mostly affected by reservoir porosity, permeability, and thickness. On the whole, the pressure increment in a reservoir of smaller porosity and permeability was greater than that in a reservoir of a greater porosity and permeability. On the other hand, the pressure increment could be decreased in a thick reservoir. The pressure increment close to the injection well was larger than that far away from the injection well. During the injection period, the pressure increment in different position of the reservoir changed with injection time and was affected by the porosity and permeability of

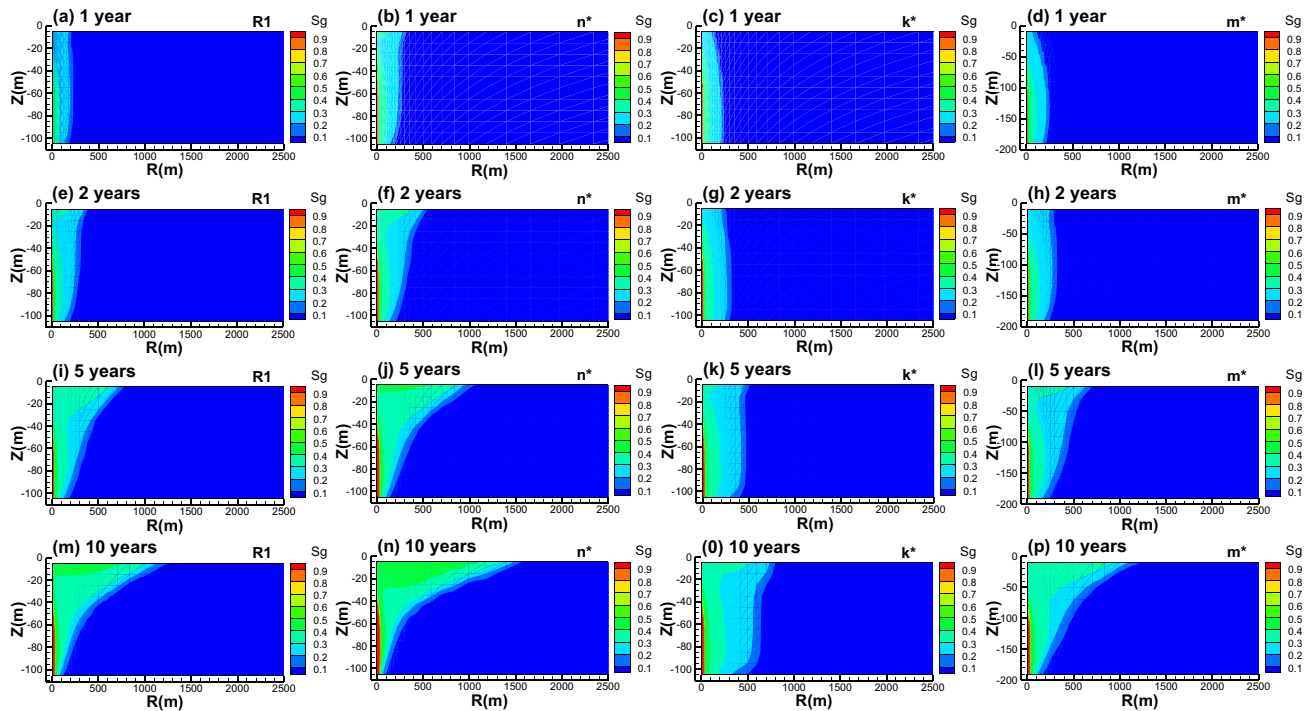


Fig. 9 Effect of reservoir porosity, permeability, and thickness on the CO₂ transport (Where n^* , k^* , and m^* , respectively, indicate the value of porosity is equal to 0.167, the value of permeability is equal to 115.9 mD, and the value of reservoir thickness is equal to 200 m)

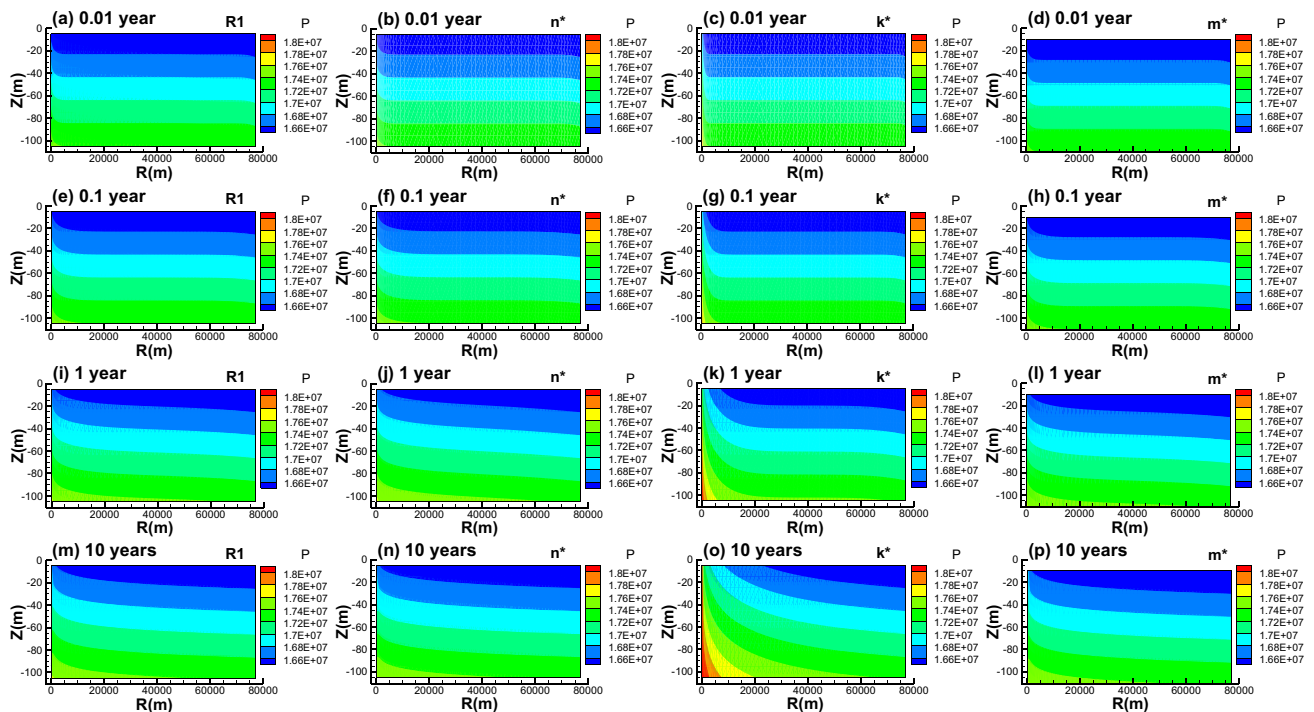


Fig. 10 Effect of reservoir porosity, permeability, and thickness on the reservoir pressure (The meanings of n^* , k^* , and m^* are the same as Fig. 9.)

the reservoir. Upon discontinuation of CO₂ injection, the reservoir pressure is restored to the original pressure.

Reservoirs with large values of porosity, permeability, and thickness are more suitable for a CO₂ geological storage with respect to CO₂ transport and pressure buildup in the reservoirs. The monitoring wells for CO₂ migration should be sited nearby the injection well (in the range of CO₂ plume distribution) and monitored not only during the injection period but also after the injection; the monitoring wells for reservoir pressure should be sited in the whole study area and monitored just during the injection period. In the particular reservoir area like the study area, CO₂ migration monitoring wells should be sited at about 20 and 2000 m away from the injection well and monitored for 1000 years as possible; reservoir pressure monitoring wells should be sited at about 20, 2000, 10000 m or far away from the injection well and monitored for 10 years.

Acknowledgments The research is sponsored by Scientific Research Foundation of Key Laboratory of Coal-based CO₂ Capture and Geological Storage, Jiangsu Province (China University of Mining and Technology) (No. 2015A05), Jiangsu Province Postdoctoral Research Funding Scheme (No. 1501155B), National Natural Science Foundation of China (41702257), the Priority Academic Program Development of Jiangsu Higher Education Institutions, the National Natural Science Foundation of China (51374203), the National Research Foundation of South Africa (RDYR160404161474), the National Basic Research Program of China (2013CB227901), and the National Natural Science Foundation of China (41502282). Thanks to the anonymous reviewers' and editor's suggestions and comments which greatly helped the authors to improve the quality of the paper.

References

- Abidoye LK, Khudaïda KJ, Das DB (2015) Geological carbon sequestration in the context of two-phase flow in porous media: a review. *Crit Rev Environ Sci Technol* 45:1105–1147. <https://doi.org/10.1080/10643389.2014.924184>
- Bachu S (2008) CO₂ storage in geological media: role, means, status and barriers to deployment. *Prog Energy Combust Sci* 34:254–273. <https://doi.org/10.1016/j.peccs.2007.10.001>
- Bachu S (2015) Review of CO₂ storage efficiency in deep saline aquifers. *Int J Greenhouse Gas Control* 40:188–202. <https://doi.org/10.1016/j.ijggc.2015.01.007>
- Beni AN, Kuehn M, Meyer R, Clauser C (2012) Numerical modeling of a potential geological CO₂ sequestration site at Minden (Germany). *Environ Model Assess* 17:337–351. <https://doi.org/10.1007/s10666-011-9295-x>
- Birkholzer JT, Zhou Q, Tsang C-F (2009) Large-scale impact of CO₂ storage in deep saline aquifers: a sensitivity study on pressure response in stratified systems. *Int J Greenhouse Gas Control* 3:181–194. <https://doi.org/10.1016/j.ijggc.2008.08.002>
- Birkholzer JT, Oldenburg CM, Zhou Q (2015) CO₂ migration and pressure evolution in deep saline aquifers. *Int J Greenhouse Gas Control* 40:203–220. <https://doi.org/10.1016/j.ijggc.2015.03.022>
- Bradshaw J, Bachu S, Bonijoly D, Burruss R, Holloway S, Christensen NP, Mathiassen OM (2007) CO₂ storage capacity estimation: issues and development of standards. *Int J Greenhouse Gas Control* 1:62–68. [https://doi.org/10.1016/s1750-5836\(07\)00027-8](https://doi.org/10.1016/s1750-5836(07)00027-8)
- Brown CJ, Poiencot BK, Hudyma N, Albright B, Esposito RA (2014) An assessment of geologic sequestration potential in the panhandle of Florida USA. *Environ Earth Sci* 71:793–806. <https://doi.org/10.1007/s12665-013-2481-1>
- Cao Y, Yuan G, Li X, Wang Y, Xi K, Wang X, Jia Z, Yang T (2014) Characteristics and origin of abnormally high porosity zones in buried Paleogene clastic reservoirs in the Shengtuo area, Dongying Sag, East China. *Pet Sci* 11:346–362. <https://doi.org/10.1007/s12182-014-0349-y>
- Chadwick RA, Noy DJ, Holloway S (2009) Flow processes and pressure evolution in aquifers during the injection of supercritical CO₂ as a greenhouse gas mitigation measure. *Pet Geosci* 15:59–73. <https://doi.org/10.1144/1354-079309-793>
- De Paz JF, Bajo J, Rodríguez S, Villarrubia G, Corchado JM (2016) Intelligent system for lighting control in smart cities. *Inf Sci* 372:241–255. <https://doi.org/10.1016/j.ins.2016.08.045>
- Du S, Su X, Xu W (2016) Assessment of CO₂ geological storage capacity in the oilfields of the Songliao Basin, northeastern China. *Geosci J* 20:247–257. <https://doi.org/10.1007/s12303-015-0037-y>
- Gislason SR, Oelkers EH (2014) Carbon storage in basalt. *Science* 344:373–374. <https://doi.org/10.1126/science.1250828>
- Guo X, Liu K, He S, Song G, Wang Y, Hao X, Wang B (2012) Petroleum generation and charge history of the northern Dongying Depression, Bohai Bay Basin, China: insight from integrated fluid inclusion analysis and basin modelling. *Mar Pet Geol* 32:21–35. <https://doi.org/10.1016/j.marpetgeo.2011.12.007>
- Hidalgo JJ, MacMinn CW, Juanes R (2013) Dynamics of convective dissolution from a migrating current of carbon dioxide. *Adv Water Resour* 62:511–519. <https://doi.org/10.1016/j.advwatres.2013.06.013>
- Jung Y, Zhou Q, Birkholzer JT (2015) On the detection of leakage pathways in geological CO₂ storage systems using pressure monitoring data: impact of model parameter uncertainties. *Adv Water Resour* 84:112–124. <https://doi.org/10.1016/j.advwatres.2015.08.005>
- Lewicki JL, Oldenburg CM, Dobeck L, Spangler L (2007) Surface CO₂ leakage during two shallow subsurface CO₂ releases. *Geophys Res Lett*. <https://doi.org/10.1029/2007gl032047>
- Li FL, Li WS (2016) Controlling factors for dawsonite diagenesis: a case study of the Binnan Region in Dongying Sag, Bohai Bay Basin, China. *Aust J Earth Sci* 63:217–233. <https://doi.org/10.1080/08120099.2016.1173096>
- Lu J, Partin JW, Hovorka SD, Wong C (2010) Potential risks to freshwater resources as a result of leakage from CO₂ geological storage: a batch-reaction experiment. *Environ Earth Sci* 60:335–348. <https://doi.org/10.1007/s12665-009-0382-0>
- Martinez-Landa L, Rotting TS, Carrera J, Russian A, Dentz M, Cubillo B (2013) Use of hydraulic tests to identify the residual CO₂ saturation at a geological storage site. *Int J Greenhouse Gas Control* 19:652–664. <https://doi.org/10.1016/j.ijggc.2013.01.043>
- Meng Q, Jiang X, Li D, Xie Q (2015) Numerical simulations of pressure buildup and salt precipitation during carbon dioxide storage in saline aquifers. *Comput Fluids* 121:92–101. <https://doi.org/10.1016/j.compfluid.2015.08.012>
- Pruess K, Oldenburg C, Moridis G (1999) TOUGH2 user's guide, Version 2.0. Lawrence Berkeley Laboratory Report LBL-43134, Berkeley, CA, USA
- Pruess K, Garcia J, Kovscek T, Oldenburg C, Rutqvist J, Steefel C, Xu TF (2004) Code intercomparison builds confidence in numerical simulation models for geologic disposal of CO₂. *Energy* 29:1431–1444. <https://doi.org/10.1016/j.energy.2004.03.077>
- Rutqvist J (2012) The geomechanics of CO₂ storage in deep sedimentary formations. *Geotech Geol Eng* 30:525–551. <https://doi.org/10.1007/s10706-011-9491-0>
- Shevalier M, Nightingale M, Mayer B, Hutcheon I (2011) TOUGHREACT modeling of the fate of CO₂ injected into a H₂S containing

- saline aquifer: the example of the Wabamun Area Sequestration Project (WASP). In: Gale J, Hendriks C, Turkenberg W (eds) 10th international conference on greenhouse gas control technologies, vol 4. Energy Procedia. pp 4403–4410. <https://doi.org/10.1016/j.egypro.2011.02.393>
- Wang YZ, Cao YC, Zhang SM, Li FL, Meng FC (2016) Genetic mechanisms of secondary pore development zones of Es (4) (x) in the north zone of the Minfeng Sag in the Dongying Depression, East China. *Pet Sci* 13:1–17. <https://doi.org/10.1007/s12182-016-0076-7>
- Xie S, Wang M (1998) Division of Palaeohydrogeological period in Dongying Sag. *Henan Pet* 12:4–7
- Xu T, Pruess K (2001) Modeling multiphase non-isothermal fluid flow and reactive geochemical transport in variably saturated fractured rocks: 1. methodology. *Am J Sci* 301(1):16–33. <https://doi.org/10.2475/ajs.301.1.16>
- Xu TF, Apps JA, Pruess K (2005) Mineral sequestration of carbon dioxide in a sandstone-shale system. *Chem Geol* 217:295–318. <https://doi.org/10.1016/j.chemgeo.2004.12.015>
- Xu TF, Sonnenthal E, Spycher N, Pruess K (2006) TOUGHREACT—a simulation program for non-isothermal multiphase reactive geochemical transport in variably saturated geologic media: applications to geothermal injectivity and CO₂ geological sequestration. *Comput Geosci* 32:145–165. <https://doi.org/10.1016/j.cageo.2005.06.014>
- Xu T, Kharaka YK, Doughty C, Freifeld BM, Daley TM (2010) Reactive transport modeling to study changes in water chemistry induced by CO₂ injection at the Frio-I Brine Pilot. *Chem Geol* 271:153–164. <https://doi.org/10.1016/j.chemgeo.2010.01.006>
- Xu T, Spycher N, Sonnenthal E, Zhang G, Zheng L, Pruess K (2011) TOUGHREACT Version 2.0: a simulator for subsurface reactive transport under non-isothermal multiphase flow conditions. *Comput Geosci* 37:763–774. <https://doi.org/10.1016/j.cageo.2010.10.007>
- Xu TF, Spycher N, Sonnenthal E, Zheng L, Pruess K (2012) TOUGHREACT user's guide: a simulation program for non-isothermal multiphase reactive transport in variably saturated geologic media, version 2.0. Lawrence Berkeley National Laboratory University of California, Berkeley
- Yang XC (1984) Geothermal features and exploration potential at depth in Dongying Depression. *Acta Pet Sin* 5(3):19–26
- Yang X (1985) An approach to the paleo-hydrogeological condition of Dongying Depression. *J China Univ Pet (Edition of Natural Science)* 64(5):812–824
- Yang D, Wang S, Zhang Y (2014) Analysis of CO₂ migration during nanofluid-based supercritical CO₂ geological storage in saline aquifers. *Aerosol Air Qual Res* 14:1411–1417. <https://doi.org/10.4209/aaqr.2013.09.0292>
- Yang Z, Niemi A, Tian L, Joodaki S, Erlstrom M (2015) Modeling of pressure build-up and estimation of maximum injection rate for geological CO₂ storage at the South Scania site, Sweden. *Greenhouse Gases-Sci Technol* 5:277–290. <https://doi.org/10.1002/ghg.1466>
- Zahid U, Lim Y, Jung J, Han C (2011) CO₂ geological storage: a review on present and future prospects. *Korean J Chem Eng* 28:674–685. <https://doi.org/10.1007/s11814-010-0454-6>
- Zhang SW, Wang YS, Shi DS, Xu HM, Pang XQ, Li MW (2004) Fault-fracture mesh petroleum plays in the Jiyang Superdepression of the Bohai Bay Basin, Eastern China. *Mar Pet Geol* 21:651–668. <https://doi.org/10.1016/j.marpetgeo.2004.03.007>
- Zhang W, Li Y, Xu T, Cheng H, Zheng Y, Xiong P (2009) Long-term variations of CO₂ trapped in different mechanisms in deep saline formations: a case study of the Songliao Basin, China. *Int J Greenhouse Gas Control* 3:161–180. <https://doi.org/10.1016/j.ijggc.2008.07.007>
- Zhang JL, Li DY, Jiang ZQ (2010) Diagenesis and reservoir quality of the fourth member sandstones of Shahejie formation in Huimin depression, eastern China. *J Cent South Univ Technol* 17:169–179. <https://doi.org/10.1007/s11771-010-0027-1>
- Zheng F, Shi XQ, Wu JC, Chen Y, Xu HX (2013) Global sensitivity analysis of reactive transport modeling of CO₂ geological storage in a saline aquifer. In: Hellmann R, Pitsch H (eds) Proceedings of the fourteenth international symposium on water-rock interaction, Wri 14, vol 7. *Procedia Earth and Planetary Science*, pp 798–801. <https://doi.org/10.1016/j.proeps.2013.03.219>
- Zhou Q, Birkholzer JT, Tsang C-F, Rutqvist J (2008) A method for quick assessment of CO₂ storage capacity in closed and semi-closed saline formations. *Int J Greenhouse Gas Cont* 2:626–639. <https://doi.org/10.1016/j.ijggc.2008.02.004>